Effect of Densification on Cellular Network Performance with Bounded Pathloss Model

Junyu Liu, Min Sheng, Lei Liu, Jiandong Li

Abstract—In this paper, we investigate how network densification influences the performance of downlink cellular network in terms of coverage probability (CP) and area spectral efficiency (ASE). Instead of the simplified unbounded pathloss model (UPM), we apply a more realistic bounded pathloss model (BPM) to model the decay of signal power caused by pathloss. It is shown that network densification indeed degrades CP when the base station (BS) density λ is sufficiently large. This is inconsistent with the result derived using UPM that CP is independent of λ. Moreover, we shed light on the impact of ultra-dense deployment of BSs on the ASE scaling law. Specifically, it is proved that the cellular network ASE scales with rate $\lambda e^{-\kappa\lambda}$, i.e., first increases with λ and then diminishes to be zero as λ goes to infinity.

I. Introduction

DUE to the simplicity and mathematical tractability, the unbounded pathloss model (UPM) $g(d) = d^{-\alpha}$[1] has been widely applied to characterize channel power gain caused by pathloss in wireless networks [1]–[3], especially when transmission distance is large in the rural areas. One exhilarating result derived using this model is that the area spectral efficiency (ASE) is monotonically increasing with the base station (BS) density in heavily loaded cellular networks [3]. However, as the network density becomes larger in the future fifth generation (5G) wireless networks, it becomes more likely that the transmission distance is small. Despite its simplicity, UPM fails to accurately characterize channel power gain in this case. In particular, when $d \in (0,1)$, applying UPM would artificially force the received signal power to be greater than the transmitted signal power, which is physically impossible.

With this regard, a more realistic model, namely, bounded pathloss model (BPM), has been adopted to model the channel power gain caused by pathloss, especially for dense urban scenarios. Widely applied BPMs include $(1+d)^{-\alpha}$, $(1+d^{\alpha})^{-1}$ and $\min(1, d^{-\alpha})$. In literature, the impact of BPM on wireless network performance has been extensively investigated [4]–[6]. In [4], authors have figured out the influence of UPM and BPM on the performance of clustered wireless ad hoc networks. To be specific, depending on the user density, it is shown that the benefits of clustering is greatly overestimated using UPM. Meanwhile, the results in [5] indicate that the probability density function (PDF) of the interference signal strength becomes heavy-tailed under UPM, while quickly decays to be zero under BPM. The difference is due to the singularity of the UPM at 0. Accordingly, compared to BPM, the application of UPM leads to significant deviations when evaluating the network performance, such as bit error

rate and wireless channel capacity, etc. However, to our best knowledge, the effect of BPM on how ASE scales with network density in cellular downlink networks remains to be explored.

In this paper, we investigate the influence of BPM on the key parameters of cellular networks, i.e., coverage probability (CP) and ASE. It is shown that CP is invariant of BS density in sparse scenarios, while is dramatically degraded by the increasing BS density when BSs are over-deployed. Based on this result, we further prove that the ASE first increases and then decreases with the BS density under BPM, which is different from the results in [3]. In addition, the optimal BS density, which leads to the largest network ASE, can be numerically obtained or be approximated in closed-form according to the analysis. The results are useful for the BS deployment and network design.

II. System Model

We consider a cellular network, which consists BSs and downlink users. Two independent homogeneous Poisson Point Processes (HPPPs), $\Pi_{\text{BS}} = \{\text{BS}_i\}$ and $\Pi_{\text{U}} = \{\text{U}_j\}$ $(i, j \in \mathbb{N})$, are used to model the locations of BSs and downlink users, respectively, in the infinitely large two-dimensional plane. A distance-based association rule has been adopted, i.e., each cellular user is connected to the geographically closest BS with constant transmit power P_{BS}. Meanwhile, we consider a heavily loaded network, in which user density is much greater than the BS density λ, such that each BS is connected with at least one user[2]. Besides, BSs are assumed to always have data to transmit.

Channel power gain is assumed to consist of a pathloss component and a distance-independent small-scale fading component. In particular, to characterize the power gain caused by pathloss, two typical BPMs are used, i.e., $g_1(d) = (1+d)^{-\alpha}$ and $g_2(d) = (1+d^{\alpha})^{-1}$, where $\alpha > 2$ denotes the pathloss exponent. Meanwhile, Rayleigh fading, $H \sim \exp(1)$, is used to model the power gain caused by small-scale fading.

Notation: Let $f_1(x)$ and $f_2(x)$ denote two functions defined on the subset of real numbers. Then, we write $f_1(x) = \Omega(f_2(x))$ if $\exists m > 0$, x_0, $\forall x > x_0$, $m|f_2(x)| \leq |f_1(x)|$ and $f_1(x) = \mathcal{O}(f_2(x))$ if $\exists m > 0$, x_0, $\forall x > x_0$, $|f_1(x)| \leq m|f_2(x)|$.

III. Coverage Probability Analysis

In this section, we investigate the performance of the downlink cellular network by evaluating the CP of a typical

---

[1]Note that d denotes the distance from the receiver to the intended transmitter.

[2]Note that each BS serves one use at one time and users are served in a round robin manner if more than one user is connected to one BS.

downlink user U_0, which is defined as

$$P_{SIR}(\lambda) = \mathbb{P}(SIR_{U_0} > \tau), \tag{1}$$

where SIR_{U_0} denotes the signal-to-interference ratio[3] (SIR) at U_0 and τ denotes the SIR threshold. Denoting d_i as the distance from BS_i to U_0, SIR_{U_0} in (1) can be expressed as

$$SIR_{U_0} = \frac{P_{BS}g_n(d_0)H_{U_0,BS_0}}{\sum\limits_{BS_i \in \Pi_{BS}^\dagger} P_{BS}g_n(d_i)H_{U_0,BS_i}}, \quad n \in \{1,2\} \tag{2}$$

where H_{U_0,BS_i} denotes the power gain caused by fading from BS_i to U_0 and $\Pi_{BS}^\dagger = \Pi_{BS} \setminus \{BS_0\}$.

In the following, we provide the CP of U_0 under BPM in Proposition 1. Note that we denote $HyF_1(x) = {}_2F_1(1, 1-\delta, 2-\delta, -x)$ and $HyF_2(x) = {}_2F_1\left(1, 1-\frac{\delta}{2}, 2-\frac{\delta}{2}, -x\right)$, where $\delta = \frac{2}{\alpha} < 1$ and ${}_2F_1(\cdot, \cdot, \cdot, \cdot)$ is the Gaussian hypergeometric function, for simplicity throughout the paper.

Proposition 1 (CP Under BMP). *Under BPMs $g_1(d) = (1+d)^{-\alpha}$ and $g_2(d) = (1+d^\alpha)^{-1}$, the CPs defined by (1) are given by (3) and (4), respectively,*

$$P_{SIR,g_1}(\lambda) = \mathbb{E}_{d_0}\left[e^{-\pi\lambda(1+d_0)(c_1(1+d_0)-c_2)}\right]$$

$$= \frac{e^{-\pi\lambda\hat{c}}}{1+c_1} + \frac{\pi\sqrt{\lambda}(c_1+\hat{c})e^{\frac{\pi\lambda(c_2^2-4\hat{c})}{4(1+c_1)}}}{2(1+c_1)^{\frac{3}{2}}}$$

$$\times \left(\text{Erfc}\left(\frac{-\sqrt{\pi\lambda}(c_1+\hat{c})}{2\sqrt{1+c_1}}\right) - 2\right), \tag{3}$$

$$P_{SIR,g_2}(\lambda) = \mathbb{E}_{d_0}\left[e^{-\frac{2\pi\lambda\tau\left(1+d_0^\alpha\right)}{(\alpha-2)d_0^{\alpha-2}}HyF_1\left(\frac{1+\tau\left(1+d_0^\alpha\right)}{d_0^\alpha}\right)}\right], \tag{4}$$

where $c_1 = \frac{2\tau HyF_1(\tau)}{\alpha-2}$, $c_2 = \frac{2\tau HyF_2(\tau)}{\alpha-1}$, $\hat{c} = c_1 - c_2$ and $\text{Erfc}(\cdot)$ denotes the complementary error function. As each user is associated with the nearest BS, the PDF of d_0 is given by $f_{d_0}(x) = 2\pi\lambda x e^{-\pi\lambda x^2}$, $x \geq 0$.

Proof: According to (1) and (2), we derive the CP as

$$P_{SIR}(\lambda) = \mathbb{P}\left(H_{U_0,BS_0} > s\sum_{BS_i \in \Pi_{BS}^\dagger} H_{U_0,BS_i}g_n(d_i)\right)$$

$$\overset{(a)}{=} \mathbb{E}_{d_0,\Pi_{BS}^\dagger, H_{U_0,BS_i}}\left[\prod_{BS_i \in \Pi_{BS}^\dagger} e^{-sH_{U_0,BS_i}g_n(d_i)}\right]$$

$$\overset{(b)}{=} \mathbb{E}_{d_0,\Pi_{BS}^\dagger}\left[\prod_{BS_i \in \Pi_{BS}^\dagger} \frac{1}{1+sg_n(d_i)}\right]$$

$$\overset{(c)}{=} \mathbb{E}_{d_0}\left[e^{-2\pi\lambda\int_{d_0}^\infty x\left(1-\frac{1}{1+sg_n(x)}\right)dx}\right], \tag{5}$$

where $s = \frac{\tau}{g_n(d_0)}$. In (5), (a) and (b) follow due to $H_{U_0,BS_0} \sim \exp(1)$ and $H_{U_0,BS_i} \sim \exp(1)$, respectively, and (c) follows due to the probability generating functional (PGFL) of Poisson point process (PPP). Replacing $g_n(d_i)$ with

---

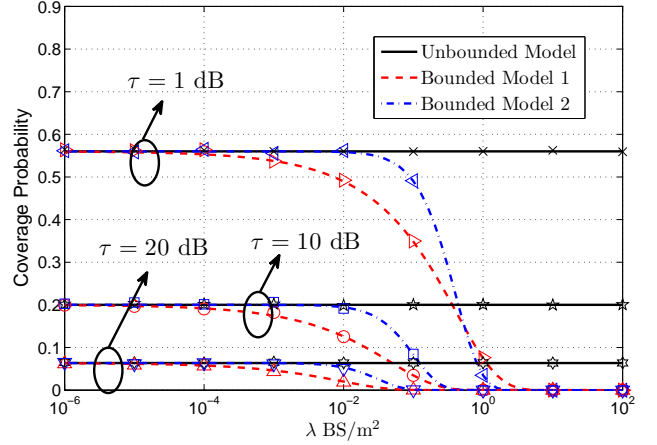[3]We ignore the impact of thermal noise on network performance, since noise is negligible in interference-limited networks.

Figure 1. CP scaling with BS density. System parameters are set as $P_{BS} = 20$ dBmW and $\alpha = 4$. Numerical results and simulation results are drawn by lines and markers, respectively.

$g_1(d_i) = (1+d_i)^{-\alpha}$ and $g_2(d_i) = (1+d_i^\alpha)^{-1}$, respectively, we complete the proof. $\square$

According to Proposition 1, we can numerically obtain the scaling law of CP. Fig. 1 plots the CP as a function of BS density varying SIR thresholds under pathloss models $g(d) = d^{-\alpha}$, $g_1(d)$ and $g_2(d)$, respectively. Note that the CP derived using $g(d)$ is obtained from the results in [3]. It is observed that the CPs are λ-invariant when λ is sufficiently small. The intuition behind this is that the increase of the received signal power is counter-balanced by the increase of interference power. Hence, the impact of λ on CP is neutralized. Furthermore, we can see that the gap between the CPs derived using BPMs and that derived using UPM is small. This indicates that UPM can accurately model the channel power gain caused by pathloss in sparse networks, where transmission distance is basically large. Nevertheless, when the network is further densified, the difference of UPM and BPM in impacting CP variation behavior becomes evident. Specifically, under BPM, the CP is greatly reduced with increasing λ (e.g., $\lambda \in [0.1, 1]$ BSs/m^2 in Fig. 1) and decays to be zero when λ is sufficiently large (e.g., $\lambda > 1$ BSs/m^2 in Fig. 1). The result manifests that user experience is significantly degraded by the over-deployment of BSs. In the next section, the influence of network densification on the network performance, i.e., network ASE, is explored.

IV. SCALING LAW OF AREA SPECTRAL EFFICIENCY

In this section, we study the network ASE and investigate the ASE scaling law. In particular, the ASE of the downlink cellular network is defined as

$$\mathcal{A} = \lambda P_{SIR}(\lambda)\log_2(1+\tau). \left[\text{bits}/\left(s\cdot Hz\cdot m^2\right)\right] \tag{6}$$

By definition, it is easy to derive the network ASE based on Proposition 1 when two typical BPMs are considered. However, since the exact results of the ASE are in complicated forms, it is difficult to directly observe how ASE scales with the BS density. To this end, we analyze the scaling law of ASE

upper bound and lower bound. Before providing the bounds of ASE, we first give the following lemma.

Lemma 1. *Denote* $F_1(x) = HyF_1(x)$ *and* $F_2(x) = \frac{HyF_1(x)}{\alpha-2} - \frac{HyF_2(x)}{\alpha-1}$ $(x \geq 0)$. *Then,* $F_1(x)$ *and* $F_2(x)$ *are monotonically decreasing functions of* x.

Proof: The monotonicity of $F_1(x)$ and $F_2(x)$ can be obtained by showing $\frac{dF_1(x)}{dx} < 0$ and $\frac{dF_2(x)}{dx} < 0$. By definition, $\frac{dF_1(x)}{dx} = -\frac{1-\delta}{2-\delta} {}_2F_1(2, 2-\delta, 3-\delta, -x)$. According to [7, Theorem 3], we have $\frac{dF_1(x)}{dx} < -\frac{1-\delta}{2-\delta} \frac{1}{\left(1+x\frac{2-\delta}{3-\delta}\right)^2} < 0$. Then, $F_1(x)$ is monotonically decreasing with x. Meanwhile, $\frac{dF_2(x)}{dx} = \frac{HyF_2(x)-HyF_1(x)}{\alpha x}$. According to [7, Theorem 1], $F_3(x) = \frac{HyF_2(x)}{HyF_1(x)}$ is a decreasing function of x, the maximum of which equals 1 when $x = 0$. Therefore, we have $HyF_2(x) < HyF_1(x)$ and $\frac{dF_2(x)}{dx} < 0$. Hence, we complete the proof. □

Based on Lemma 1, we study the upper/lower bounds of ASE under BPMs in the following proposition.

Proposition 2 (ASE Upper/Lower Bound Under BMPs). *Under BPMs* $g_1(d) = (1+d)^{-\alpha}$ *and* $g_2(d) = (1+d^\alpha)^{-1}$, *the network ASE is upper bounded by* $\mathcal{A}^{\mathrm{U}}(\lambda) = \lambda\log_2(1+\tau)\frac{e^{-\pi\lambda 2^{-\alpha}\hat{c}}}{1+2^{-\alpha}\hat{c}}$ *and lower bounded by* $\mathcal{A}^{\mathrm{L}}(\lambda)$

$$
= \lambda\log_2(1+\tau)\left[\frac{e^{-\pi\lambda(1+2^\alpha c_1)}}{1+2^{\alpha-2}c_1} \right.
$$
$$
\left. - \frac{2^{\alpha-2}c_1\pi\sqrt{\lambda}e^{-\frac{\pi\lambda c_1 2^{\alpha-2}}{1+2^{\alpha-2}c_1}}\mathrm{Erfc}\left(\frac{\sqrt{\pi\lambda}\left(1+2^{\alpha-1}c_1\right)}{\sqrt{1+2^{\alpha-2}c_1}}\right)}{(1+2^{\alpha-2}c_1)^{\frac{3}{2}}}\right] \quad (7)
$$

Proof: When $g_n(d)$ is replaced by $g_1(d) = (1+d)^{-\alpha}$, we obtain the lower bound of CP based on (3) as

$$
\mathsf{P}_{\mathrm{SIR},g_1}(\lambda) \overset{(a)}{>} \mathbb{E}_{d_0}\left[e^{-\pi\lambda c_1(1+d_0)^2}\right]
$$
$$
= \frac{e^{-\pi\lambda c_1}}{1+c_1} - \frac{e^{-\frac{\pi\lambda c_1}{1+c_1}}\pi\sqrt{\lambda}c_1}{(1+c_1)^{\frac{3}{2}}}\mathrm{Erfc}\left(\frac{\sqrt{\pi\lambda}c_1}{\sqrt{1+c_1}}\right)
$$
$$
= \mathsf{P}_{\mathrm{SIR},g_1}^{\mathrm{L}}(\lambda), \quad (8)
$$

where (a) follows due to the fact that $c_1(1+d_0) - c_2 < c_1(1+d_0)$ since $c_2 > 0$, and e^{-x} is a decreasing function of x. Next, we obtain the upper bound of CP as

$$
\mathsf{P}_{\mathrm{SIR},g_1}(\lambda) \overset{(a)}{<} \mathbb{E}_{d_0}\left[e^{-\pi\lambda\hat{c}(1+d_0)^2}\right]
$$
$$
= \frac{e^{-\pi\lambda\hat{c}}}{1+\hat{c}} - \frac{e^{-\frac{\pi\lambda\hat{c}}{1+\hat{c}}}\pi\sqrt{\lambda}\hat{c}}{(1+\hat{c})^{\frac{3}{2}}}\mathrm{Erfc}\left(\frac{\sqrt{\pi\lambda}\hat{c}}{\sqrt{1+\hat{c}}}\right)
$$
$$
= \mathsf{P}_{\mathrm{SIR},g_1}^{\mathrm{U}}(\lambda), \quad (9)
$$

where (a) follows because $c_1(1+d_0) - c_2 > c_1(1+d_0) - c_2(1+d_0)$ in (3) and e^{-x} is a decreasing function of x.

When $g_n(d)$ is replaced by $g_2(d) = (1+d^\alpha)^{-1}$, the CP in

(1) turns into

$$
\mathsf{P}_{\mathrm{SIR},g_2}(\lambda_{\mathrm{BS}}) = \mathbb{P}\left(\frac{P_{\mathrm{BS}}H_{\mathrm{U}_0,\mathrm{BS}_0}g_2(d_0)}{\sum_{\mathrm{BS}_i\in\Pi_{\mathrm{BS}}^\dagger}P_{\mathrm{BS}}H_{\mathrm{U}_0,\mathrm{BS}_i}g_2(d_i)} > \tau\right).
$$

Since $g_1(d) < g_2(d)$, we derive the lower bound of CP by weakening the useful signal power received at BS_0 using the BPM $g_1(d_0)$. Accordingly, we have

$$
\mathsf{P}_{\mathrm{SIR},g_2}(\lambda) > \mathbb{P}\left(\frac{P_{\mathrm{BS}}H_{\mathrm{U}_0,\mathrm{BS}_0}g_1(d_0)}{\sum_{\mathrm{BS}_i\in\Pi_{\mathrm{BS}}^\dagger}P_{\mathrm{BS}}H_{\mathrm{U}_0,\mathrm{BS}_i}g_2(d_i)} > \tau\right)
$$
$$
\overset{(a)}{=} \mathbb{E}_{d_0}\left[e^{-\frac{2\pi\lambda\tau(1+d_0)^\alpha}{(\alpha-2)d_0^{\alpha-2}}}HyF_1\left(\frac{1+\tau(1+d_0^\alpha)}{d_0^\alpha}\right)\right]
$$
$$
\overset{(b)}{>} \mathbb{E}_{d_0}\left[e^{-\frac{\pi\lambda c_1(1+d_0)^\alpha}{d_0^{\alpha-2}}}\right]
$$
$$
> \mathbb{E}_{d_0}\left[e^{-\frac{\pi\lambda c_1(1+d_0)^\alpha}{d_0^{\alpha-2}}}\Big|d_0\in[1,\infty)\right]
$$
$$
\overset{(c)}{\geq} \mathbb{E}_{d_0}\left[e^{-\pi\lambda c_1(1+d_0)^\alpha\left(\frac{1+d_0}{2}\right)^{2-\alpha}}\Big|d_0\in[1,\infty)\right]
$$
$$
= \mathsf{P}_{\mathrm{SIR},g_2}^{\mathrm{L}}(\lambda) < \mathsf{P}_{\mathrm{SIR},g_1}^{\mathrm{L}}(\lambda). \quad (10)
$$

In (10), the derivation step of (a) is similar to those in (5), (b) follows because $F_1(x) = HyF_1(x)$ is a decreasing function of x according to Lemma 1 and (c) follows because $d_0^{2-\alpha} \leq \left(\frac{1+d_0}{2}\right)^{2-\alpha}$ when $d_0 \in [1,\infty)$. Similarly, we weaken the interference signal power received at BS_0 by replacing $g_2(d_i)$ with $g_1(d_i)$. Hence, the CP upper bound can be obtained as follows

$$
\mathsf{P}_{\mathrm{SIR},g_2}(\lambda)
$$
$$
< \mathbb{P}\left(\frac{P_{\mathrm{BS}}H_{\mathrm{U}_0,\mathrm{BS}_0}g_2(d_0)}{\sum_{\mathrm{BS}_i\in\Pi_{\mathrm{BS}}^\dagger}P_{\mathrm{BS}}H_{\mathrm{U}_0,\mathrm{BS}_i}g_1(d_i)} > \tau\right)
$$
$$
= \mathbb{E}_{d_0}\left[e^{-\frac{2\pi\lambda s_2}{(1+d_0)^{\alpha-2}}\left(\frac{HyF_1\left(\frac{s_2}{(1+d_0)^\alpha}\right)}{\alpha-2} - \frac{HyF_2\left(\frac{s_2}{(1+d_0)^\alpha}\right)}{\alpha-1}\right)}\right]
$$
$$
\overset{(a)}{<} \mathbb{E}_{d_0}\left[e^{-\pi\lambda\hat{c}(1+d_0^\alpha)(1+d_0)^{2-\alpha}}\right]
$$
$$
\overset{(b)}{<} \mathbb{E}_{d_0}\left[e^{-\pi\lambda\hat{c}\frac{(1+d_0)^\alpha}{2^\alpha}(1+d_0)^{2-\alpha}}\right]
$$
$$
< \mathbb{E}_{d_0}\left[e^{-\pi\lambda\hat{c}\frac{1+d_0^2}{2^\alpha}}\right]
$$
$$
= \mathsf{P}_{\mathrm{SIR},g_2}^{\mathrm{U}}(\lambda) > \mathsf{P}_{\mathrm{SIR},g_1}^{\mathrm{U}}(\lambda), \quad (11)
$$

where (a) follows because $F_2(x) = \frac{HyF_1(x)}{\alpha-2} - \frac{HyF_2(x)}{\alpha-1}$ is a decreasing function of x according to Lemma 1 and (b) follows due to $1+d_0^\alpha \geq \left(\frac{1+d_0}{2}\right)^\alpha$. Combining the results in (8), (9), (10) and (11), we complete the proof. □

Based on Proposition 2, we characterize the scaling law of the ASE using the following theorem.

Theorem 1 (ASE Scaling Under BMP). *Under the BPMs* $g_1(d) = (1+d)^{-\alpha}$ *and* $g_2(d) = (1+d^\alpha)^{-1}$, *network ASE scales with rate* $\lambda e^{-\kappa\lambda}$, *where* κ *is a constant.*

Proof: The result is obtained by proving that $\mathcal{A}^L(\lambda) = \Omega\left(\lambda e^{-\pi\lambda(1+2^\alpha c_1)}\right)$ and $\mathcal{A}^U(\lambda) = \mathcal{O}\left(\lambda e^{-\pi\lambda 2^{-\alpha}\hat{c}}\right)$. According to Proposition 2, it is obtained that $\left|\mathcal{A}^U(\lambda)\right| \leq \lambda\log_2(1+\tau) e^{-\pi\lambda 2^{-\alpha}\hat{c}}$. Therefore, it can be shown that $\mathcal{A}^U(\lambda) = \mathcal{O}\left(\lambda e^{-\pi\lambda 2^{-\alpha}\hat{c}}\right)$. Then, considering the ASE lower bound, we have $\left|\mathcal{A}^L(\lambda)\right| \geq \frac{\lambda\log_2(1+\tau)}{1+2^{\alpha-2}c_1}(Q_1(\lambda) - Q_2(\lambda))$, where $Q_1(\lambda) = e^{-\pi\lambda(1+2^\alpha c_1)}$ and $Q_2(\lambda) = \frac{2^{\alpha-2}\pi c_1\sqrt{\lambda}e^{-\frac{\pi\lambda c_1 2^{\alpha-2}}{1+c_1 2^{\alpha-2}}}}{\sqrt{1+2^{\alpha-2}c_1}}\mathrm{Erfc}\left(\frac{\sqrt{\pi\lambda}(c_1 2^{\alpha-1}+1)}{\sqrt{c_1 2^{\alpha-2}+1}}\right)$. Through showing $\exists\lambda_0 > 0$, $\forall\lambda > \lambda_0$, $\frac{Q_2(\lambda)}{Q_1(\lambda)} \in \left(0, \frac{1}{2}\right)$, we have $\left|\mathcal{A}^L(\lambda)\right| \geq \frac{\lambda\log_2(1+\tau)}{2(1+2^{\alpha-2}c_1)}Q_1(\lambda)$. Hence, $\forall\lambda > \lambda_0$, $\left|\mathcal{A}^L(\lambda)\right| \geq \frac{\log_2(1+\tau)}{2(1+2^{\alpha-2}c_1)}\left|\lambda e^{-\pi\lambda(1+2^\alpha c_1)}\right|$. Therefore, we have $\mathcal{A}^L(\lambda) = \Omega\left(\lambda e^{-\pi\lambda(1+2^\alpha c_1)}\right)$. □

It is shown from Theorem 1 that the network ASE first increases and then decreases with λ. On the one hand, network densification greatly improves spatial reuse by reducing the distance between transmitters and receivers. On the other hand, network over-densification pushes too many interfering BSs around downlink users, which incurs severe inter-cell interference. Therefore, when the spatial resources are fully exhausted, the benefits of spatial reuse vanish and the detriment of network densification overwhelms, thereby degrading network ASE. More importantly, the results demonstrate the importance of using BPM to characterize channel power gain, considering the ultra-dense deployment of BSs.

Fig. 2 plots the ASE scaling with BS density. It can be seen that the network performance is overestimated using UPM, as the resulting ASE is always greater than that derived using BPM. The reason is that the application of UPM artificially amplifies the useful signal power at $d \in (0,1)$. Meanwhile, we observe that the exact results derived using the two BPMs decay with λ at the same rate with those derived using the upper/lower bound. This indicates the validity of Theorem 1. Additionally, we interestingly find that the optimal λ^*, which maximizes the system ASE, can be approximated using the densities λ_U^* that maximize the ASE upper bound $\mathcal{A}_{g_1}^U(\lambda) = \lambda\log_2(1+\tau)\mathsf{P}_{\mathrm{SIR},g_1}^U(\lambda)$, where $\mathsf{P}_{\mathrm{SIR},g_1}^U(\lambda)$ is given by (9). Note that λ_U^* can be derived in closed-form by solving $\frac{d\mathcal{A}_{g_1}^U(\lambda)}{d\lambda} = 0$. Therefore, the impact of system parameters on λ^* can be directly observed, which provides guidance for the deployment of BSs.

V. Conclusion

In this paper, we show that the cellular network ASE scales with rate $\lambda e^{-\kappa\lambda}$ when BPM is used to characterize pathloss. According to the scaling law, network densification cannot alway boost the network capacity especially when BS density is sufficiently large. This differs from the traditional understanding that cellular network ASE scales linearly with λ. Meanwhile, the closed-form expression of the density, which leads to the inflection of the ASE, can be approximated.
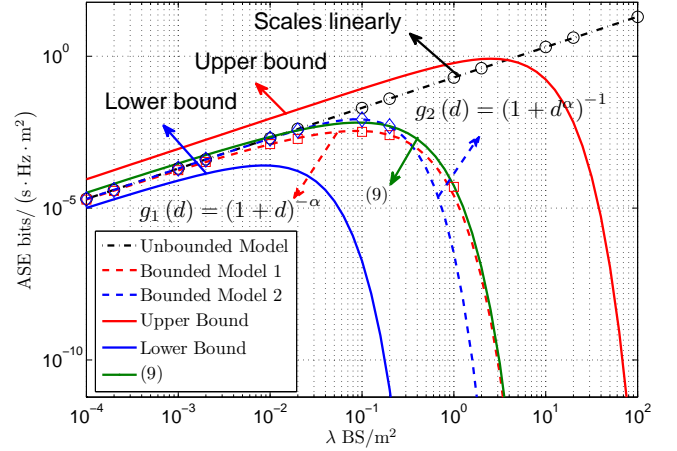

Figure 2. ASE scaling with BS density. System parameters are set as $P_{\mathrm{BS}} = 20\,\mathrm{dBmW}$, $\tau = 10\,\mathrm{dB}$ and $\alpha = 4$. Numerical results and simulation results are drawn by lines and markers, respectively.

The result is helpful to understand how network parameters affect the network scaling law, thereby providing guideline for the efficient deployment of cellular networks.

It is worth noting that the single-slope BPM used throughout the paper cannot characterize the discrepant power decay levels within different regions, which is caused by non-line-of-sight (NLOS) and line-of-sight (LOS) propagation of the signal. Recently, the influence of NLOS and LOS transmissions on dense network performance, e.g., CP and ASE, has been evaluated and proved to be significant in [8], [9]. Nonetheless, the impact of singularity has not been fully explored therein. Therefore, future study should consider the multiple pathloss model, which is defined based on BPM. Following this approach, the influence of network densification on the network capacity would become valid and convincing.

References

[1] A. Guo and M. Haenggi, "Spatial stochastic models and metrics for the structure of base stations in cellular networks," *IEEE Trans. Wireless Commun.*, vol. 12, no. 11, pp. 5800–5812, Nov. 2013.

[2] H. ElSawy and E. Hossain, "On stochastic geometry modeling of cellular uplink transmission with truncated channel inversion power control," *IEEE Trans. Wireless Commun.*, vol. 13, no. 8, pp. 4454–4469, Aug. 2014.

[3] H. S. Dhillon, R. K. Ganti, F. Baccelli, and J. G. Andrews, "Modeling and analysis of K-Tier downlink heterogeneous cellular networks," *IEEE J. Sel. Areas Commun.*, vol. 30, no. 3, pp. 550–560, Apr. 2012.

[4] R. K. Ganti and M. Haenggi, "Interference and outage in clustered wireless ad hoc networks," *IEEE Trans. Inf. Theory*, vol. 55, no. 9, pp. 4067–4086, Sep. 2009.

[5] H. Inaltekin, M. Chiang, H. V. Poor, and S. B. Wicker, "On unbounded path-loss models: effects of singularity on wireless network performance," *IEEE J. Sel. Areas Commun.*, vol. 27, no. 7, pp. 1078–1092, Sep. 2009.

[6] H. Inaltekin, "Gaussian approximation for the wireless multi-access interference distribution," *IEEE Trans. Signal Process.*, vol. 60, no. 11, pp. 6114–6120, Nov. 2012.

[7] D. Karp and S. Sitnik, "Inequalities and monotonicity of ratios for generalized hypergeometric function," *Journal of Approximation Theory*, vol. 161, no. 1, pp. 337–352, Nov. 2009.

[8] X. Zhang and J. G. Andrews, "Downlink cellular network analysis with multi-slope path loss models," *IEEE Trans. Commun.*, vol. 63, no. 5, pp. 1881–1894, May 2015.

[9] M. Ding, P. Wang, D. Lopez-Perez, G. Mao, and Z. Lin, "Performance impact of LoS and NLoS transmissions in dense cellular networks," *IEEE Trans. Wireless Commun.*, vol. 15, no. 3, pp. 2365–2380, Mar. 2016.